Available online at www.sciencedirect.com

SciVerse ScienceDirect

Energy Procedia 10 (2011) 225 – 231

Energy Procedia

European Materials Research Society Conference
Symp. Advanced Inorganic Materials and Concepts for Photovoltaics

Charge transfer from CdTe quantum dots into a CdS thin layer

Elisabeth Zillner, Björn Eckhardt, Ahmed Ennaoui, Martha Ch. Lux-Steiner, Thomas Dittrich a*

Helmholtz-Zentrum Berlin für Materialien und Energie GmbH, Hahn-Meitner Platz 1, 14109 Berlin, Germany

Abstract

Electron injection from CdTe quantum dots (CdTe-QDs) into ultra-thin CdS layers has been demonstrated by transient and spectral dependent surface photovoltage (SPV) methods while the thickness of the CdS layer was varied systematically between several nm and tens on nm. Signal heights and decay times at half maximum were correlated with the thickness of the CdS layer. The decay times increased by several orders of magnitude for electrons transferred across the charge-selective CdS/CdTe-QD contact in comparison to electrons photo-generated in the CdS layer.

quantum dots ; surface photovoltage ; CdTe ; CdS

1. Introduction

Highly absorbing semiconductors such as CdTe, CdSe or In_2S_3/In_2S_3:Cu deposited at low temperatures are of interest for solar cells with extremely thin absorber, in which the local absorber layer thickness is less than the transport length [1-3]. Nanoparticle layers of highly absorbing semiconductors open new options for conditioning of nano-structured solar cells and can broaden the strategic potential of

* Corresponding author. Tel.: +49-30-8062 42090; fax: +49-30-8062 43199.
E-mail address: thomas.dittrich@helmholtz-berlin.de

 doi:10.1016/j.egypro.2011.10.182

semiconducting materials for solar energy conversion [4]. For example the increase of the absorption edge of PbS or PbSe using the quantum size effect can be used in quantum dot (QD) based solar cells [5-6]. Further, charge selective, Ohmic and passivating contacts may be engineered by using nanoparticle or QD layers. For example, charge separation has been demonstrated by surface photovoltage (SPV) methods for type II hetero-junctions based on CdSe-QD / CdTe-QD systems [7]. QDs bear also the opportunity to overcome the Shockley-Queisser limit of energy conversion [8] by making use of multi-exciton generation [9]. However, charge-selective contacts to layers of semiconductor nanoparticles are still challenging. In this work, charge separation in system of ultra-thin CdS compact layers covered with CdTe nanoparticles has been investigated by transient SPV and by spectral dependent modulated SPV. The CdS layers were deposited by the ion layer gas reaction (ILGAR) [10] method allowing well defined layer thicknesses and conformal coating from solution.

2. Experimental

Layers of CdS were deposited by ILGAR on glass substrate coated with SnO_2:F (TEC15) in the same manner as described recently [11]. The samples were successively dipped in 0.04 M $Cd(ClO_4)_2$ solution in acetonitrile, dried in N_2 flow, sulfurized in Ar/H_2S flow at 160°C, cooled in N_2 flow and washed in THF. One ILGAR cycle corresponded to a CdS layer thickness of 1-2 nm. The numbers of ILGAR cycles were 1, 3, 6, 10 and 20 for the different samples. CdTe nanoparticles (diameter 8 nm, pyridine surfactants, provided by Bayer Technology Services GmbH, figure 1a) in pyridine suspension (4 mg/g) were spin coated at an angular speed of 2000 rpm on the samples and dried at 200 °C for 10 min. The samples were not completely covered by CdTe nanoparticles (see figure 1b), the average thickness of CdTe nanoparticles was of the order of one monolayer. The samples were named CdS-0/CdTe-np, CdS-1/CdTe-np, CdS-3/CdTe-np, CdS-6/CdTe-np, CdS-10/CdTe-np, and CdS-20/CdTe-np for zero, 1, 3, 6, 10, and 20 ILGAR cycles of CdS deposition, respectively.

Transient and modulated spectral dependent SPV measurements were performed in the fixed capacitor arrangement [12]. The fixed capacitor was formed by the SnO_2:F back contact with the semiconductor layer, a mica spacer and an SnO_2:F front contact deposited on a quartz cylinder, via which illumination was performed. SPV signals were detected via a high impedance buffer with an oscilloscope (GAGE CompuScope 14200) or with a double phase lock-in (Signal Recovery Model 5210) for transient or modulated excitation, respectively.

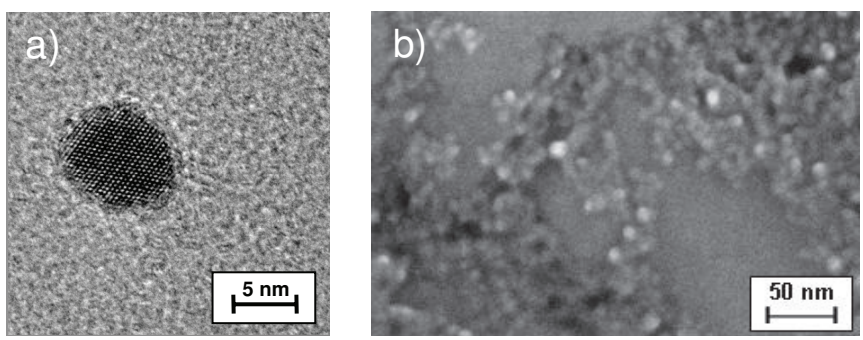

Fig. 1. (a) Transmission electron microscopy image of a CdTe quantum dot. (b) Secondary electron microscopy view of a CdS surface prepared by ILGAR and partially covered with CdTe nanoparticles.

Laser excitation wavelengths of 700 nm (absorption in CdTe; band gap = 1.45 eV [13]) and 500 nm (absorption in CdTe and CdS; band gap = 2.47 eV [14]), at intensities of 1.7 mJ/cm^2 and 4.7 mJ/cm^2, respectively were applied for the measurements of transients. The resolution time was limited for short times by the pulse length of the exciting laser pulse (5 ns, EKSPLA, NT343/1/UVE) and the oscilloscope and for long times by the RC time constant (10…100 ms) of the sample capacitance and the measurement resistance of 10 GΩ. Transients were recorded on a logarithmic scale between 10 ns (corresponding to 100MS/s) and 0.1 s.

Modulated illumination (chopping frequency 5 Hz) for spectral measurements was done via a halogen lamp and a monochromator with a quartz prism (Carl Zeiss Jena 408069). The SPV signals for modulated excitations were recorded in phase (U_X) and phase shifted by $\pi/2$ (U_Y) with respect to the chopped light. The U_Y signal characterizes the shift in time between the illumination and the SPV signal, whereas U_X displays the fast SPV response. The data in this publication are represented in the amplitude U_R and the phase φ, while the amplitude is given by $U_R = (U_X^2 \cdot U_Y^2)^{1/2}$ and the phase by $\tan\varphi = U_X / U_Y$.[12] Thus the phase contains information about the time characteristic of the SPV signal and the mechanism of charge separation in the sample. A phase angle of 0° means that photo-generated electrons are separated towards the internal interface while charge separation and recombination are much faster than the modulation period. At the other side, a phase angle of 180° means a fast separation of photo-generated electrons towards the external surface together with fast recombination. Shifts of the phase angles towards -90° or 90° mean that charge separation and recombination become remarkable or even slow in relation to the modulation period.

3. Results and discussion

3.1. Transient SPV measurements

Figure 2a shows SPV transients of the samples CdS-(0,1,6,10,20)/CdTe-np excited below the band gap of CdS. The SPV signal was negative for the sample CdS-0/CdTe-np with a maximum SPV of -16 mV. This means that photo-generated electrons were separated preferentially towards the external surface for a layer of CdTe nanoparticles deposited on bare SnO_2:F. The sign of the SPV transient remained negative for sample CdS-1/CdTe-np but the maximum SPV decreased to -3 mV. The coverage of the samples with CdTe nanoparticles did not depend on the number of ILGAR cycles. Therefore the strong decrease of the SPV signal for sample CdS-1/CdTe-np in comparison to sample CdS-0/CdTe-np gave evidence for the appearance of a competitive mechanism of charge separation. The SPV signals changed their sign to positive for samples with more than 1 cycle of CdS ILGAR deposition, while the positive maximum SPV signal increased with increasing number of ILGAR cycles. This means that the competitive mechanism of charge separation became dominant with increasing thickness of the CdS layer.

The dependence of the SPV signal at 100 ns on the number of ILGAR cycles is plotted in figure 2b for excitation wavelength of 700 nm. The behavior of the points at 1, 3, 6, 10 and 20 cycles could be linearly fitted with a slope of 1.6 mV/cycle and an intersection with y-axis at -3 mV, i.e. the SPV signal scaled linearly with the thickness of the CdS layer. Further the amount of charge carriers photo-generated in CdTe-np remained constant since the coverage of CdS with CdTe-np was independent of the number of ILGAR cycles. Hence injection of photo-generated electrons from CdTe-np into the CdS layer was the dominating mechanism of charge separation for CdS-(1, 3, 6,10, 20)/CdTe-np samples.

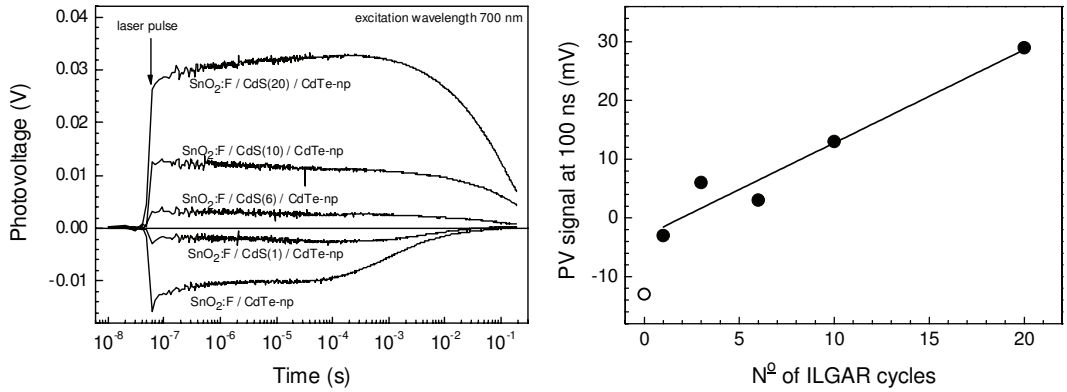

Fig. 2. (a) Surface photovoltage transients of SnO2:F coated with CdTe nanoparticles and of SnO2:F coated with CdS (1, 6, 10 and 20 ILGAR cycles) and CdTe nanoparticles. The transients were excited at a wavelength of 700 nm. (b) Dependence of the SPV signal at 100 ns on the number of ILGAR cycles (excitation wavelength 700 nm).

The SPV signals decayed with time or remained nearly constant over a relatively long time for all samples, except sample CdS-20/CdTe-np excited at 700 nm. The SPV transient of sample CdS-20/CdTe-np excited at 700 nm increased in time and reached the maximum of 33 mV at a time of about 0.2 ms. The increase of the SPV signal with time gives evidence for a slow increase of the charge separation length in time due to diffusion [15] with a very low effective diffusion coefficient (of the order of 10^{-8} cm²/s for diffusion of electrons limited by defect states).

Transients of the CdS-20/CdTe-np sample excited at 700 nm and 500 nm are compared in figure 3a. The maximum SPV signal excited at 500 nm is about one order of magnitude larger than the maximum SPV signal excited at 700 nm. This increase was caused by strong photo-generation in the CdS layer for excitation at 500 nm. The behavior of both transients was quite different. The transient excited at 500 nm had a fast component whereas both transients had a slow component with a decay time of the order of 0.1 s given by the discharge of the measurement capacitor via the large measurement resistance. The SPV transients could not be fitted with a certain function. For this reason the times at which the SPV signal decayed to half maximum were compared (figure 3b).

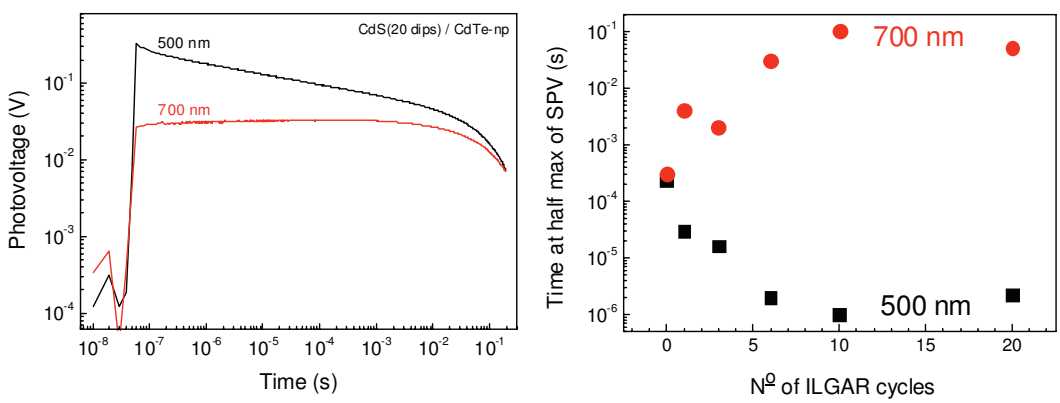

Fig. 3. (a) Surface photovoltage transients of SnO_2:F coated with CdS (20 ILGAR cycles) and CdTe nanoparticles at excitation wavelengths of 500 and 700 nm (thin and thick lines, respectively). (b) Dependence of the decay time at half maximum as a function of the number of ILGAR cycles for excitation wavelengths of 500 (squares) and 700 nm (circles).

For excitation at 700 nm the decay times increased from about 0.2 ms to 0.1 s with increasing number of ILGAR cycles. In contrast the decay times decreased to about 1 µs with increasing number of ILGAR cycles for excitation at 500 ns. This means that the lifetime of electrons injected from CdTe-np into the CdS layer was very long, hence recombination of electrons injected into CdS and holes remaining in the CdTe-np was strongly suppressed by the CdTe-np/CdS hetero-junction, while a thickness of the CdS layer of the order of 10-20 nm was sufficient.

3.2. Spectral dependent SPV

Figure 4a depicts the amplitude spectra of modulated SPV for the investigated samples. The spectrum of the exciting light intensity is shown for comparison. The strong decrease of the amplitudes at photon energies above 3.6 eV was caused by absorption in the SnO_2:F front electrode via which the samples were illuminated. The signature of the band gap of CdTe can be clearly seen for all spectra. Interestingly the PV amplitude was very similar at photon energies around 1.6 eV for all samples excepting CdS-6/CdTe-np for which the PV amplitude was about 7-8 times lower. The signature of the band gap of CdS became apparent for the CdS-6/CdTe-np sample and strong for CdS-10,20/CdTe-np samples.

The spectra of the PV amplitude were nearly identical for samples CdS-0,1,3/CdTe-np for photon energies above the band gap of CdTe. Signatures of the band gap of CdS could not be observed in these spectra. The samples differ in the PV amplitudes for photon energies below the band gap of CdTe, while the lowest PV amplitude was measured for sample CdS-1/CdTe-np in this range.

There were significant SPV signals at photon energies below the band gap of CdTe. A detailed analysis of the SPV signals below 1.4 eV was not possible due to the behavior of the lamp spectrum and due to the fact that SPV amplitudes can not be simply normalized to a photon flux as one can do for photocurrent spectra. The strongest contribution to modulated charge separation was observed for defect states in the forbidden band gap of samples CdS-0/CdTe-np (about 50 µV at 1.3 eV) and CdS-20/CdTe-np (about 30 µV at 1.3 eV), while the SPV signal set on at lower photon energies for sample CdS-20/CdTe-np. The lowest contribution to modulated charge separation was observed for defect states in the forbidden band gap of sample CdS-10/CdTe-np (about 4 µV at 1.3 eV). The suppression of modulated charge separation from defect states was related to the competition of mechanisms of charge separation contributing to the SPV with different signs.

For the CdS-20/CdTe-np sample the signal below 1.4 eV was about three orders of magnitude smaller than the maximum amplitude. To check for an infrared sensitivity of the sample a Si wafer was placed in front of the monochromator as a filter for visible light. Measuring at photon energies of 0.6 eV, with the Si wafer as filter, no SPV signal was observed. Thus the signal observed at low photon energies could be ascribed to the influence of stray light in the monochromator. The part of the stray light on our samples was in the range of 0.1 % and was out of our measurement sensitivity for all samples except the CdS-20/CdTe-np sample.

The phase spectra of modulated SPV are given in figure 4b for all samples investigated. The phase of the modulated SPV spectra contains information about the direction and time of charge separation and recombination (see chapter experimental for detailed discussion). The phase spectrum of sample CdSe-0/CdTe-np was close to 180° over the whole spectrum while the band gap of CdTe could be detected as a little dip in the phase spectrum. This means that separation of photo-generated electrons towards the external surface and their recombination was fast and practically independent of the origin of excitation for CdTe-np deposited at bare SnO2:F. For samples CdS-1/CdTe-np and CdS-3/CdTe-np the phase spectra were practically identical over the whole spectral range and equal to the phase spectrum of sample CdS-0/CdTe-np for photon energies above the band gap of CdTe. There was no signature for the band gap of CdS at all in these spectra. Therefore, despite transient SPV, modulated SPV was not influenced

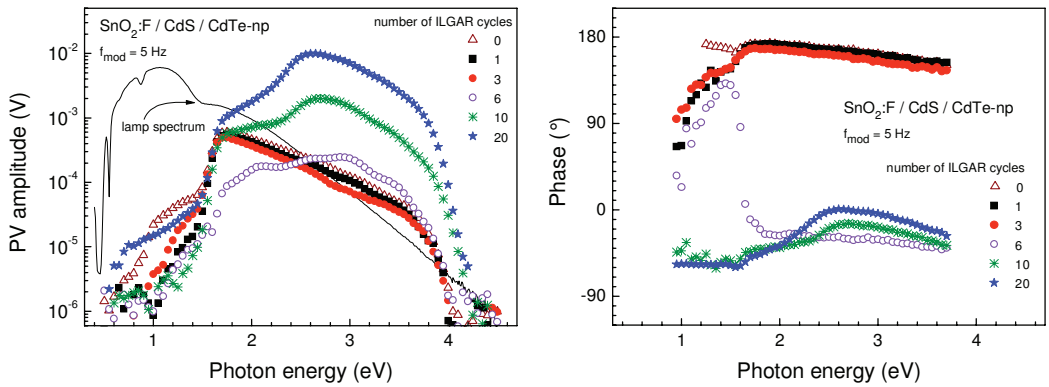

Fig. 4. (a) Amplitude spectra on a logarithmic scale and (b) phase spectra of modulated surface photovoltage for SnO_2:F coated with CdTe nanoparticles (triangles) and for SnO_2:F coated with CdS (1, 3, 6, 10 and 20 ILGAR cycles, squares, filled circles, open circles, crosses and stars, respectively) and CdTe nanoparticles. The black line shows the spectrum of the halogen lamp.

by CdS for deposition of 1 and 3 ILGAR cycles. This was caused by the very slow recombination of electrons injected from CdTe into CdS in contrast to much faster recombination of photo-generated electrons separated towards the external surface of the CdTe-np layer. Since the phase angle was very close to 180° it can be concluded that the charge separation observed for these samples is related to intra-particle charge transfer in CdTe-np.

The phase angles of sample CdS-6/CdTe-np at photon energies below the band gap of CdTe were still quite similar (bit lower) to the spectra of samples CdS-1/CdTe-np and CdS-3/CdTe-np, i.e. charge separation from defect states was still dominated by charge transfer within the CdTe-np. However, the phase angle changed from 130° at 1.45 eV to values around -25° for photon energies above 1.85 eV, i.e. photo-generated electrons were separated towards the internal interface.

The phase angles of samples CdS-10/CdTe-np and CdS-20/CdTe-np were about -60° in the spectral range from 0.9 to 1.6 eV, i.e. both sample had an identical mechanism of modulated charge separation in the defect range. For photon energies above 1.6 eV the phase angles increased to -15° and 0° at 2.6 eV for samples CdS-10/CdTe-np and CdS-20/CdTe-np, respectively. For photon energies above 2.6 eV the phase angles became more negative again. Therefore for the thicker CdS layers coated with CdTe-np the mechanisms of charge separation and recombination changed depending on the photon energy. This was not surprising if taking into account, for example, strongly decreasing distant dependent recombination with increasing charge separation length and a strong dependence of charge transport on the free electron and hole concentrations. As remark, accumulation of free charge carriers took place due to the very slow component of recombination in relation to the modulation period.

4. Conclusions

A charged-selective CdTe/CdS contact was formed by spin coating of CdTe-QDs onto CdS solid thin films. Thus a change from intra-particle charge transport to transport across the nanoparticle/CdS interface was realized. Charge carriers separated across the interface display a long lifetime ($\geq$0.1 s) compared to charge carries separated within the quantum dot (0.3 ms). Furthermore charge separation from defect states of the CdTe-QD was suppressed by the CdS.

Acknowledgements

The work was supported by the BMBF (grant: 03SF0363B). The authors are grateful to Dr. K. Köhler and Dr. F. Rauscher (Bayer Technology Services GmbH) for the supply of CdTe nanoparticles. Acknowledgements to Jaison Kavalakkatt and Ulrike Blöck for the measurements of SEM and TEM pictures.

References

[1] Ernst K, Belaidi A, Könenkamp R. Solar cell with extremely thin absorber on highly structured substrate. *Semicond. Sci. Technol.* 2003;**18**:475–9

[2] Tena-Zaera R, Katty A, Bastide S, Lévy-Clément C, O´Regan B, Muñoz-Sanjosé V. ZnO/CdTe/CuSCB, a promising heterostructure to act as inorganic *eta*-solar cell. *Thin Solid Films* 2005;**483**:372-7.

[3] Belaidi A, Dittrich Th, Kieven D, Tornow J, Schwarzburg K, Lux-Steiner M. Influence of the local absorber layer thickness on the performance of ZnO nanorod solar cells. *phys. stat. sol. (RRL)* 2008;**4**:172-4.

[4] Wadia C, Alivisatos AP, Kammen DM. Materials Availability Expands the Opportunity for Large-Scale Photovoltaics Deployment. *Environ. Sci. Technol.* 2009;**43**:2072–7.

[5] Pattantyus-Abraham AG, Kramer IJ, Barkhouse AR, Wang X, Konstantatos G, Debnath R, et al. Depleted-Heterojunction Colloidal Quantum Dot Solar Cells. *ACS NANO* 2010;**4**, 3374.

[6] Luther MJ, Law M, Beard MC, Song Q, Reese MO, Ellingson RJ, et al. Schottky Solar Cells Based on Colloidal Nanocrystal Films. *Nano Letters* 2008;**8**:3488-92

[7] Gross D, Mora-Sero L, Dittrich Th, Belaidi A, Mauser C, Houtepen A, et al. Charge Separation in Type II Tunneling Multilayered Structures of CdTe and CdSe Nanocrystals Directly Proven by Surface Photovoltage Spectroscopy. *Am. Chem. Soc.* 2010;**132**:5981-3.

[8] Shockley W, Queisser HJ. Detailed Balance Limit of Efficiency of p-n Junction Solar Cells. *Journal of Applied Physics* 1961;**32**:510-9

[9] Klimov VI. Mechanisms for Photogeneration and Recombination of Multiexcitons in Semiconductor Nanocrystals: Implications for Lasing and Solar Energy Conversion. *J. Phys. Chem. B* 2006;**110**:16827-45

[10] Muffler H-J, Fischer Ch-H, Diesner K, Lux-Steiner M. ILGAR - A novel thin-film technology for sulfides. *Solar Energy Materials & Solar Cells* 2001;**67**:121-7

[11] Dittrich Th, Bönisch S, Zabel P, Dube S. High precision differential measurement of surface photovoltage transients on ultrathin CdS layers. *Review of Scientific Instruments* 2008;**79**:113903

[12] Duzhko V, Timushenko VY, Koch F, Dittrich Th. Photovoltage in nanocrystalline porous TiO_2. Phys. Rev. B 2001;**64**:075204

[13] Dietrich A, Bube J, Bube RH. Semiconducting Cadmium Telluride. *Phys Rev* 1954;**96**:1190-1

[14] Sankar N, Sanjeeviraja C, Ramachandran K. Growth and characterization of CdS and doped CdS single crystals. *Journal of Crystal Growth* 2002;**243**:117-23

[15] Mora-Seró I, Dittrich Th, Garcia-Belmonte G, Bisquert J. Determination of spatial charge separation of diffusing electrons by transient photovoltage measurements. *J. Appl. Phys.* 2006;**100**:103705